Deep machine learning interatomic potential for liquid silica

I. A. Balyakin [1,2] S. V. Rempel [3,2] R. E. Ryltsev [1,4,5] and A. A. Rempel [1,2]

[1] *Institute of Metallurgy of the Ural Branch of the Russian Academy of Sciences, 620016, Ekaterinburg, Russia*

[2] *Ural Federal University, NANOTECH Centre, 620002, Ekaterinburg, Russia*

[3] *Institute of Solid State Chemistry of the Ural Branch of the Russian Academy of Sciences, 620145 Ekaterinburg, Russia*

[4] *Vereshchagin Institute for High Pressure Physics, Russian Academy of Sciences, 108840 Troitsk, Moscow, Russia*

[5] *Ural Federal University, Engineering School of Information Technologies, Telecommunications and Control Systems, 620002, Ekaterinburg, Russia*

(Received 7 July 2020; accepted 13 October 2020; published 23 November 2020)

The use of machine learning to develop neural network potentials (NNP) representing the interatomic potential energy surface allows us to achieve an optimal balance between accuracy and efficiency in computer simulation of materials. A key point in developing such potentials is the preparation of a training dataset of *ab initio* trajectories. Here we apply a deep potential molecular dynamics (DeePMD) approach to develop NNP for silica, which is the representative glassformer widely used as a model system for simulating network-forming liquids and glasses. We show that the use of a relatively small training dataset of high-temperature *ab initio* configurations is enough to fabricate NNP, which describes well both structural and dynamical properties of liquid silica. In particular, we calculate the pair correlation functions, angular distribution function, velocity autocorrelation functions, vibrational density of states, and mean-square displacement and reveal a close agreement with *ab initio* data. We show that NNP allows us to expand significantly the time-space scales achievable in simulations and thus calculating dynamical and transport properties with more accuracy than that for *ab initio* methods. We find that developed NNP allows us to describe the structure of the glassy silica with satisfactory accuracy even though no low-temperature configurations were included in the training procedure. The results obtained open up prospects for simulating structural and dynamical properties of liquids and glasses via NNP.

DOI: 10.1103/PhysRevE.102.052125

I. INTRODUCTION

Application of machine learning (ML) in simulations of materials is an actively developed paradigm. The main idea behind such techniques is to fit properly the interatomic potential energy surface (PES) of a particle system using some reference data, which are usually provided by *ab initio* simulations. Since pioneering works at the end of the 2000s [1–3], a number of closely related ML approaches have been proposed so far to solve this problem and applied successfully for studying condensed matter systems of different nature [3–20]. These methods can be divided into three main families: the linear regression methods, such as the spectral neighbor analysis method [14,19] and the moment tensor potentials [20]; kernel methods, including Gaussian approximation potential method [3,18] and its modifications [5,6]; and different approaches based on deep neural networks [7–13,21–23]. Despite common ideas and purposes, these methods may differ essentially by the manner in which they fit a PES. The neural network approach seems one of the most general and promising, at least for simulating bulk materials. Neural network potentials (NNPs) fit a PES as a complex nonlinear function of local environment descriptors, which must be invariant under translation, rotation, and permutation of atoms. There are many NNPs proposed so far, such as deep potential molecular dynamics (DeePMD) [7–10], neural network potential package (n2p2) [11,12], accurate neural artificial intelligence network engine for molecular energies (ANI) [21,22], and deep learning architecture for molecules and materials by K. T. Schütt (SchNet) [23]. They are based on similar ideas but utilize different sets of local descriptors and different configurations of fitting neural networks. Anyway, properly designed NNP can provide nearly *ab initio* accuracy with orders of magnitude less computational cost [10–12].

One the most obvious applications of NNPs is the molecular dynamics simulations of liquids. Indeed, NNPs allows us to simulate thousands of particles at the timescales of nanoseconds, which is enough for an accurate description of both structural and dynamical properties of a liquid. Thus NNPs give us a unique ability for calculating transport properties of materials with nearly *ab initio* accuracy as well as studying large-scale structural properties. Note that due to the novelty of NNP approach its application to the liquid state description has not yet been thoroughly validated.

A key issue in developing NNPs is the preparation of a training dataset of *ab initio* configurations that represent properly the PES of a system in a certain domain of configurational space. In most cases, training configurations are obtained by *ab initio* molecular dynamics (AIMD) simulations performed using density-functional theory. Such calculations are very time-consuming and so the search for effective ways to generate optimal training datasets is an important task in the context of computational cost. Another issue is the possibility of using NNPs to describe thermodynamic states that are far

from those included in the training dataset. It is obvious, that this possibility depends strongly on how much the structure of the system varies under change of thermodynamic conditions. The answer to this issue is especially important in the context of simulations of supercooled liquids and glasses for which obtaining properly relaxed AIMD configuration is an extremely difficult task.

Here we address these issues for silica, which is of great practical importance as a material for the semiconductor industry [24], pharmacy [25], food industry [26], and nanotechnology [27]. Nano- and micro-sized silica particles serve as a base for fabricating colloidal suspensions, which are the main objects in studying self-assembly and tunable interactions [28–30]. Moreover, silica is the representative glassformer widely used as a model system in studying network-forming liquids and glasses [31–41]. Due to its practical and fundamental importance, there have been intensive researches in the field of computer simulations of silica. Thus, a lot of interatomic potentials for this system have been developed [42–46]. However, the NNP model combining the accuracy of AIMD and the efficiency of classical simulations has not been developed so far. Here we introduce such NNPs, which have been trained and tested using a DeePMD kit [7–9,47,48]. By using the training dataset of high-temperature AIMD configurations for relatively small systems of 96 atoms, we fabricate NNP, which describes well both structural and dynamical properties of liquid silica. Then, this NNP was used to generate statistically independent configurations for creating more reliable dataset, which was used for improvement of the initial NNP. We find that this new NNP also allows us to describe the structure of the glassy silica with satisfactory accuracy even though no low-temperature configurations have been included in the training procedure.

II. METHODS

A. *Ab initio* calculations

The training datasets for NNP were generated by AIMD simulations utilizing density-functional theory as implemented in Vienna *ab initio* simulation program [49]. Projector augmented-wave pseudopotentials and Perdew-Burke-Ernzerhof (PBE) [50,51] gradient approximation to the exchange-correlation functional were used [52]. Only the Γ point was used to sample the Brillouin zone and the energy cutoff of 500 eV was set, which is higher than the default cutoff automatically obtained from pseudopotentials. A Nose-Hoover thermostat was used to control the temperature.

Two training *ab initio* datasets were generated. The first one was created based on AIMD simulations of systems containing 96 particles. The initial configurations for AIMD were generated by classical molecular dynamics simulations with Tersoff potential as implemented in LAMMPS code [53]. The initial configuration for classical simulations was created as a cubic lattice of 96 atoms (32 atoms of Si and 64 atoms of O) which was randomly distributed over the lattice sites. This structure was melted and annealed at 5000 K and zero pressure $P = 0$ for 10 ps. Then we collected five substantially different configurations, which were used as the initial ones for independent AIMD runs performed in stepwise manner at (5000, 4500,. . . , 2000) K; the final state at higher temperature was used as the initial state for the lower temperature. At each temperature, the systems were relaxed for 20 ps (10 000 steps of 2 fs) and when equilibrium data were collected for another 20 ps; the volume for all AIMD runs was equal to the equilibrium volume at $P = 0$, $T = 5000$ K. The timestep was 2 fs and all the configuration were saved in the training dataset. Note that all the AIMD configurations (even the nonrelaxed ones) were included in the training procedure. But, for the calculation of the observable properties, only the equilibrium configurations were used. Thus, the total number of configuration was $5 \times 7 \times 10\,000 = 350\,0000$, which were divided into training and testing subsets in the ratio of 2:1. This dataset was used to train NNP, which will be further referred to as DeePMD-96.

The second dataset was generated for 216 particle systems using different strategy. Here we utilized DeePMD-96 to generate three long trajectories that contained 10^6 MD steps of 2 ps at $T = 3000$, 4000, and 5000 K. Then we collected 100 configurations with the step of 5000 frames from each trajectory and used them as initial configurations for independent AIMD runs of 100 steps of 1 fs. Since the main purpose for creating this dataset was the better description of the glassy structure (see Sec. III A), all calculations were performed at the same volume corresponding to experimental room-temperature density of glassy silica. Thus, the dataset contained 30 000 configurations of 216 atoms. This dataset was used to develop NNP, which will be further referred to as DeePMD-216.

B. Training procedure

To develop NNP for silica, we mainly use a DeePMD package [7–9,47,48]. To validate the results, the alternative NNP was trained with the same datasets by using n2p2 code developed by Singraber and coworkers [11] based on an approach proposed earlier by Behler and Parrinello [1,12]. Both methods utilize feedforward multilayer neural networks (perceptrons) as fitting functions. The main difference between them is the set of local environment descriptors, which are fed to the input layer of the neural network to provide invariance under translation, rotation, and permutation. In the smooth version of DeePMD we used (DeepPot-SE) [48], end-to-end smooth and continuous embedding network is used for that purpose, which allows us to transform properly the atomic coordinates in a rather automatic manner. In the n2p2 method, the set of so-called symmetry functions have to be properly specified. Both methods give almost the same results but DeePMD demonstrates a more convenient and user-friendly procedure for preparing training data. Moreover, n2p2-based simulations more often demonstrate unstable behavior when the system falls out the ranges of values of the symmetry functions that were obtained during the training procedure. This problem is probably caused by the fact that the chosen set of symmetry functions fails to describe some local atomic environments. Thus, a very careful tuning of the symmetry functions is needed. As a result, n2p2 approach requires more routine work to obtain the same results than DeePMD. Hereinafter, we will discuss only the results obtained by DeePMD.

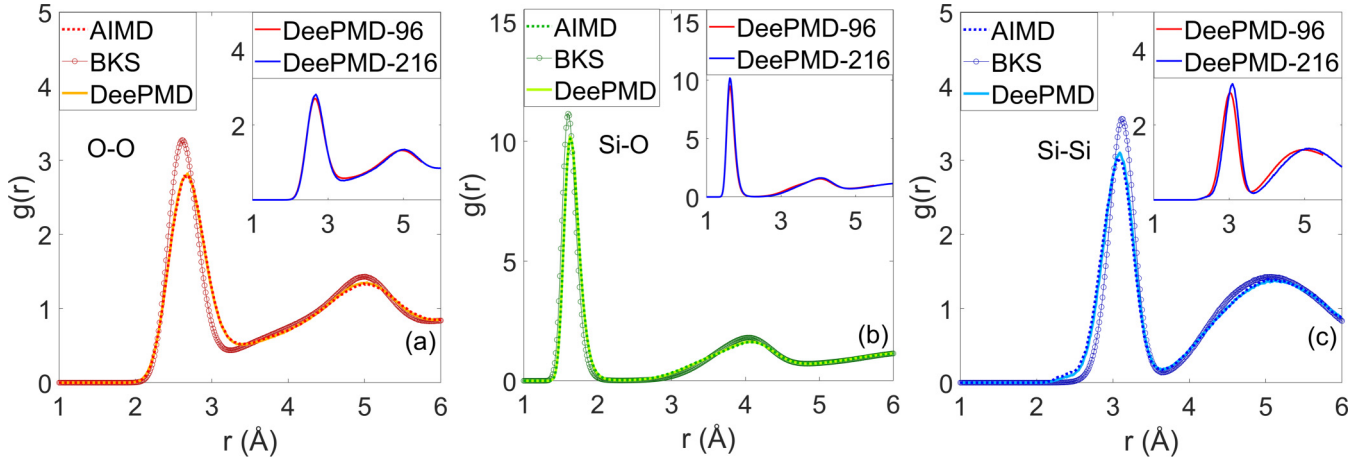

FIG. 1. Main frame: Partial O-O, Si-O, and Si-Si radial distribution functions $g(r)$ for liquid silica at $T = 3000$ K calculated via AIMD, NNP (DeePMD-216), and BKS potential. All calculations are performed at $N = 216$. Insets: The comparison between RDFs calculated by DeePMD-96 and DeePMD-216.

The cutoff radius $r_{\rm cut}$ of DeepPot-SE model was set to 6.0 Å and descriptors decay smoothly from 4.5 Å to the $r_{\rm cut}$. The sizes of the angle filter, radial filter, and fitting networks were {10, 20, 40}, {5, 10, 20}, and {40, 20, 10}, respectively. The decay rate and decay step were set to 0.95 and 5000, respectively. For DeePMD-96, the prefactors in the loss functions were $p_e^{\rm start} = 1.00$, $p_e^{\rm limit} = 1.00$, $p_f^{\rm start} = 100$, and $p_f^{\rm limit} = 100$. For DeePMD-216, we set $p_e^{\rm start} = 1.00$, $p_e^{\rm limit} = 10.0$, $p_f^{\rm start} = 1000$, and $p_f^{\rm limit} = 100$. No virial data were included in the training process in both cases and so we set $p_v^{\rm start} = 0$, $p_v^{\rm limit} = 0$.

C. NNP simulations

The DeePMD kit includes implementation to the LAMMPS code, which allows us to perform direct MD simulations with the developed NNP. In order to compare correctly the results obtained by NNP and AIMD calculations, we apply the same simulation conditions in both cases. In particular, all the NNP results presented below in comparison with AIMD was obtained for the systems containing either $N = 96$ (for DeePMD-96) or $N = 216$ (for DeePMD-216) particles to eliminate possible difference in the finite-size effects. NNP simulations were performed in the temperature interval 3000–5000 K in a stepwise manner using a final frame of each run as an initial configuration for the next one. Each simulation contained 10^5 (10^6) MD steps for DeePMD-96 (DeePMD-216). When calculating observable properties, we excluded the first 10% of MD configurations to obtain equilibrium structures. To fabricate a glassy structure of silica, we considered the system of 2592 atoms (864 SiO_2 units) for DeePMD-96 and 5832 atoms (1944 SiO_2 units) for DeePMD-216. These systems were quenched from 3000 K down to 300 K with the cooling rate of 10^{12} K/s. Then, the quenched structure was annealed at 300 K for 10^4 MD steps to calculate structural characteristics, which can be compared with available experimental neutron scattering data. The length of MD step during quenching from 3000 K to 1500 was equal to 1.5 fs; in all other cases, it was 1.0 fs. In all cases, the Nose-Hoover thermostat with damping parameter 100 fs was used to control the temperature.

III. RESULTS AND DISCUSSION

A. Structural properties

We start our discussion with the comparison of the structural characteristics calculated via AIMD, NNP, and van Beest-Kramer-Santen (BKS) potential [46], which is one of the most widely used classical force fields for silica. The first resort method in studying the structure of liquids is the analysis of the radial distribution function (RDF) $g(r)$. In Fig. 1 we show partial RDFs of liquid silica at $T = 3000$ K calculated via the methods mentioned above. We see from the Fig. 1 that NNP provide excellent agreement with AIMD data. Comparison to BKS potential reveal qualitatively the same behavior with noticeable quantitative differences. Remember, that we use two versions of NNP, DeePMD-96 and DeePMD-216. The former was constructed from *ab initio* trajectories obtained for 96 particle system and the latter is a second-family NNP constructed from a large number of statistically independent AIMD trajectories whose initial configurations were generated by DeePMD-96. In the main frames of Fig. 1, we show the results obtained using DeePMD-216. A comparison between DeePMD-96 and DeePMD-216 is presented in the insets and reveals small differences. However, DeePMD-216 provides slightly better agreement with AIMD, especially for Si-Si pairs. As we will see below, the difference between the two NNPs is more substantial in the description of the glassy state (see Fig. 3). In general, presented RDFs reveal strong chemical interaction between species, especially for Si-O pairs. That is in agreement with our knowledge about the interatomic interactions in silica.

Another widely used distribution function providing important information about structural correlations beyond RDF is the bond angle distribution function (BADF), which is the probability density for an angle between two vectors connected the target atom with its two nearest neighbors. Partial BADFs for silica at $T = 3000$ K are shown in Fig. 2. We see again that BADFs calculated via AIMD and NNP are in very good agreement. The comparison between BADF calculated via two versions of NNP presented in the inset reveals almost the same results. In general, BADFs calculated demonstrate

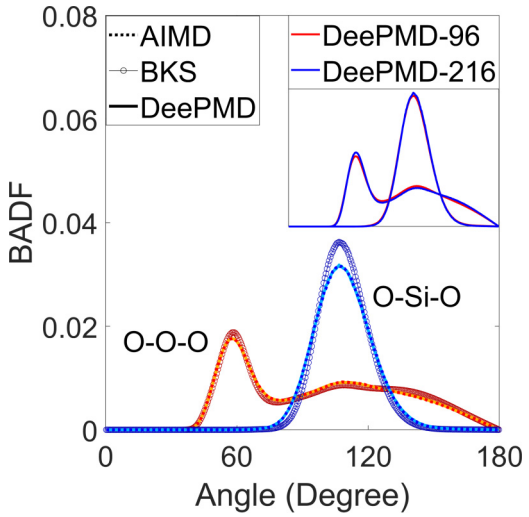

FIG. 2. Main frame: Partial BADFs for liquid silica at $T = 3000$ K calculated via AIMD, NNP (DeePMD-216), and BKS potential. All calculations are performed at $N = 216$. Insets: The comparison between BADFs calculated by DeePMD-96 and DeePMD-216.

the picture corresponding to the tetrahedral structure of the liquid silica. Indeed, the locations of the first maxima in O-O-O and O-Si-O distributions correspond to almost perfect silicon-centered tetrahedron with the oxygen atoms in its vertexes.

Thus, we see that developed NNP provides good accuracy in describing the structure of liquid silica. On the one hand, this is rather expectable result because NNP under consideration was developed using liquid *ab initio* trajectories. On the other hand, this result is important in the context that neural networks are able to fit PES for network-forming systems with strongly anisotropic interactions.

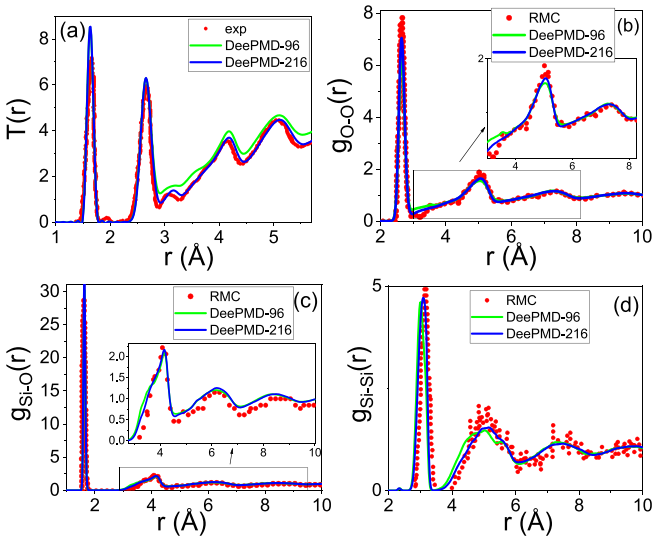

FIG. 3. Pair correlation function (a) and partial radial distribution functions [(b)–(d)] for the vitreous silica. The red bullets in panels (a) and (b)–(d) represent respectively the data obtained by neutron diffraction [54] and those calculated from experimental data by the reverse Monte Carlo method [55]. The solid lines in all panels correspond to NNP simulations. DeePMD-96 (green) and DeepMD-216 (blue) represent respectively the results obtained with NNPs, which were trained using *ab initio* data for $N = 96$ and $N = 216$ particle systems. The insets in panels (b) and (c) show the areas marked by rectangles on a larger scale.

A much more difficult task is the description of the vitreous silica structure by using NNPs. Correct solution of this problem requires including in the training dataset atomic configurations corresponding to supercooled liquid and glassy states. However, an implicit generation of such configurations via AIMD is hardly possible because the timescales, which are achievable in simulations, are not enough to equilibrate the structure of a particle system at relatively low temperatures. Thus, the development of NNPs for describing supercooled liquid and glasses, is an challenging task, which is beyond the scopes of this work.

Here we address the particular issue on this way: How closely a NNP developed via high-temperature liquid configurations describes the structure of glassy silica? To answer this question for the NNPs under consideration, we plot in Fig. 3 pair correlation function for the vitreous silica obtained by neutron diffraction [54] as well as partial radial distribution functions calculated from experimental data by the reverse Monte Carlo method [55] and compare them with the results of NNP simulations. For the sake of comparison, the results obtained using both versions of NNP (DeePMD-96 and DeePMD-216) are presented. We see that the NNPs describe satisfactory the structure of the glassy state in spite of the facts that (1) no glassy configurations were included in the training dataset and (2) the cooling rate of 10^{12} K/s applied in simulations to obtain the glassy state is of orders of magnitude higher than that in experiments. It is important to note that DeePMD-216 demonstrates much better agreement with experimental data. That may be explained by the following reasons: (1) the dataset applied to train the DeePMD-216 model contains more statistically independent configurations and thus more effectively covers the configurational space of the system and (2) the larger system is less affected by finite-size effect, which can be important in the glassy state.

The relative success of the NNP in describing glass structure is probably due to the special network structure of silica, which does not change qualitatively during the cooling. In the systems like metallic alloys, where the structure changes essentially at cooling, one might expect that NNP trained on high-temperature configurations would fail describing the glassy state. Of course, even in the case of silica under consideration, additional efforts are necessary to achieve a better description of the glassy state. First, the training dataset should be extended by adding properly generated glassy configurations [8,56–58]. Second, the properties of numerically quenched systems can substantially depend on the cooling rate [59–62] and so more sophisticated methods like swap Monte Carlo [63–65] or sub-T_g annealing [59,60] should be utilized to obtain a more realistic glassy structure.

B. Dynamical properties

We have seen above that NNPs developed provide a good description of structural properties of the silica. Here we focus on dynamical properties (dynamic correlation functions),

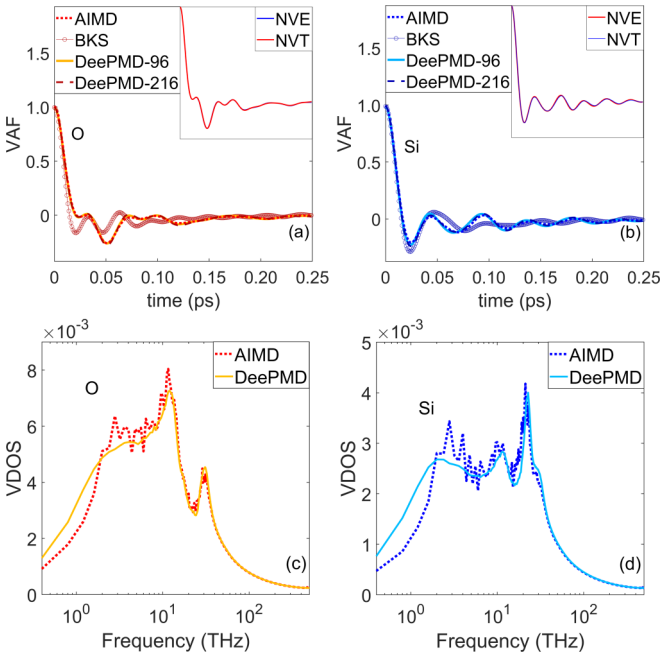

FIG. 4. [(a) and (b)] Partial VAFs for liquid silica at $T = 3000$ K calculated via AIMD, NNP, and BKS potential at the number of particles $N = 96$. Insets compare VAFs extracted from NVE and NVT ensemble simulations. [(b) and (c)] Vibrational densities of states obtained via Fourier transform of VAF. Calculations were performed at $N = 96$ for AIMD and $N = 2592$ for DeePMD-96. We see that, due to larger system size, DeePMD allows us to calculate VDOS with much higher accuracy.

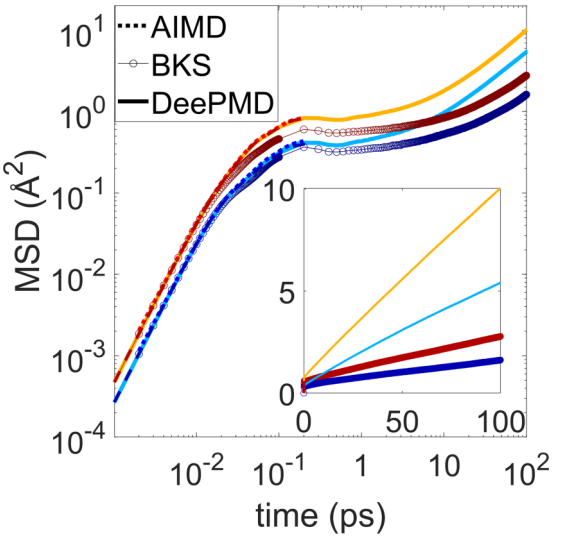

FIG. 5. Main frame: MSD of liquid silica at $T = 3000$ K calculated via AIMD, DeePMD, and BKS potential. We see that DeepMD allows us to cover timescales corresponding to diffusion regime in atomic motion, whereas AIMD does not. Inset: MSD curves in linear scale, which demonstrate clearly the linear behavior at $t \gg 0$.

whose calculation requires much more precision in the description of interatomic forces than in the case of structural characteristics.

The simplest but important dynamical correlation function is the velocity autocorrelation function (VAF), which is the correlator of particle velocity,

$$Z(t) = \langle \mathbf{v}(t) \cdot \mathbf{v}(0) \rangle,$$

where averaging is performed over particle trajectories. The practical importance of VAF is that (i) its Fourier transform presents the density of vibrational states [66] and (ii) Green-Kubo relation with VAF gives the exact mathematical expression for diffusion coefficient [67]. Note that we will always use VAF normalized on its initial value.

In Figs. 4(a) and 4(b) we show partial VAFs for liquid silica at $T = 3000$ K calculated via AIMD, NNP, and BKS potential. We see again that NNP provides excellent agreement with *ab initio* data. Interestingly that BKS potential, even though it describes satisfactorily the structural properties, demonstrates only qualitative (not quantitative) agreement with AIMD in describing VAF.

Since the use of a thermostat can affect the atomic dynamics, we perform NVE ensemble simulations, calculate VAF and compare it with that obtained in NVT [see insets in Figs. 4(a) and 4(b)]. The results are practically the same that suggests the influence of the Nose-Hoover thermostat is negligible in our case.

Note that, for the sake of accurate comparison, we calculate VAF by all methods using the same conditions as for AIMD [$N = 96$ (or 216), $t_{\max} = 0.2$ ps]. However, the big advantage of NNPs is that they allow us to expand significantly the time-space scales achievable in simulations. That is especially relevant for calculating dynamical characteristics. In Figs. 4(c) and 4(d) we illustrate this fact by the example of the calculation of vibrational density of states (VDOS) via Fourier transform of VAF. In this case, when calculating VDOS by DeePMD, we consider a larger system of $N = 2592$ particles. That allows us to achieve much higher accuracy in calculating VDOS in comparison to AIMD.

Another important dynamic correlation function is the mean-square displacement (MSD). In the condensed matter theory, MSD is widely used for calculations of the diffusion coefficients via the Einstein relation as well as an indicator of glassy dynamics [68–70]. In Fig. 5 we show MSD for liquid silica calculated at $T = 3000$ K by the methods under consideration. As for VAF, NNP demonstrates an excellent description of MSD, whereas BKS provides only qualitative accuracy. Note that the MSDs presented in Fig. 5 reveal behavior, which is typical for glass-forming liquids including liquid silica [39,71]. Namely, there are three detectable dynamical regimes: the ballistic regime at short times, the plateau at intermediate timescales, and the long-time linear (diffusion) regime [39,68]. Besides, at the crossover between ballistic and plateau regimes (at around 0.2 ps) a little bump is detected. This is the distinctive feature of the silica, which is sometimes related to the boson peak [39].

It is important that AIMD simulations performed in reasonable computer time allows us to cover only the first two regimes; two orders of magnitude longer simulations are needed to get diffusion regime. Such simulations are extremely time-consuming for even small system sizes, which means it is hardly possible to calculate the transport properties of viscous liquids like silica by using AIMD. At the same time, NNP approach allows us to perform simulations at

hydrodynamic space-time scales and so calculating transport properties with high accuracy. This fact is one of the most fascinating capabilities of ML-based approaches.

IV. CONCLUSIONS

We utilize a deep machine learning approach as implemented in DeePMD kit to develop NNP, which represents properly the PES of silica. We focus on studying a liquid state but also obtain some preliminary results for a glass.

Using only high-temperature liquid AIMD trajectories in the training dataset, we develop a NNP, which provides nearly *ab initio* accuracy in describing structural and dynamical correlation functions of liquid silica, such as radial distribution function, bond-angle distribution function, velocity autocorrelation function, and mean-square displacement. Structural properties of the glassy state are also described with satisfactory accuracy in spite of the fact that no glassy data were included in the training procedure.

We have also proposed an iterative procedure for developing NNPs. The main idea is to achieve iterative self-consistent improvement of a NNP by creating a dataset to train children-NNP using statistically independent initial configurations generated by means of parent-NNP. For silica, this procedure does not affect significantly the properties of a liquid but leads to essential improvements in the description of the glassy state.

Our findings suggest that NNPs allows us to achieve high-enough accuracy in describing both structural and dynamical properties of network-forming liquids and can be considered a promising tool for studying supercooled liquid and glasses.

ACKNOWLEDGMENTS

This work was mainly performed within the state assignment of the Institute of Solid State Chemistry of the Ural Branch of the Russian Academy of Sciences (Grant No. 0397-2019-0001) and Institute of Metallurgy of the Ural Branch of the Russian Academy of Sciences. R.R. was supported by the Russian Science Foundation (Grant No. 18-12-00438). The numerical calculations are carried out using computing resources of "Uran" cluster of IMM UB RAS [72]. We thank N. Chtchelkatchev for valuable discussion.

[1] J. Behler and M. Parrinello, Phys. Rev. Lett. **98**, 146401 (2007).
[2] J. Behler, R. Martoňák, D. Donadio, and M. Parrinello, Phys. Rev. Lett. **100**, 185501 (2008).
[3] A. P. Bartók, M. C. Payne, R. Kondor, and G. Csányi, Phys. Rev. Lett. **104**, 136403 (2010).
[4] T. Mueller, A. Hernandez, and C. Wang, J. Chem. Phys. **152**, 050902 (2020).
[5] R. Jinnouchi, F. Karsai, and G. Kresse, Phys. Rev. B **100**, 014105 (2019).
[6] R. Jinnouchi, J. Lahnsteiner, F. Karsai, G. Kresse, and M. Bokdam, Phys. Rev. Lett. **122**, 225701 (2019).
[7] L. Zhang, D.-Y. Lin, H. Wang, R. Car, and W. E, Phys. Rev. Materials **3**, 023804 (2019).
[8] T. Wen, C.-Z. Wang, M. J. Kramer, Y. Sun, B. Ye, H. Wang, X. Liu, C. Zhang, F. Zhang, K.-M. Ho, and N. Wang, Phys. Rev. B **100**, 174101 (2019).
[9] L. Zhang, J. Han, H. Wang, R. Car, and W. E, Phys. Rev. Lett. **120**, 143001 (2018).
[10] Y. Zhang, H. Wang, W. Chen, J. Zeng, L. Zhang, H. Wang, and W. E, Comput. Phys. Commun. **253**, 107206 (2020).
[11] A. Singraber, J. Behler, and C. Dellago, J. Chem. Theory Comput. **15**, 1827 (2019).
[12] J. Behler, J. Chem. Phys. **145**, 170901 (2016).
[13] K. T. Schütt, F. Arbabzadah, S. Chmiela, K. R. Müller, and A. Tkatchenko, Nat. Commun. **8**, 13890 (2017).
[14] A. Thompson, L. Swiler, C. Trott, S. Foiles, and G. Tucker, J. Comput. Phys. **285**, 316 (2015).
[15] T. D. Huan, R. Batra, J. Chapman, S. Krishnan, L. Chen, and R. Ramprasad, npj Comput. Mater. **3**, 37 (2017).
[16] E. V. Podryabinkin and A. V. Shapeev, Comput. Mater. Sci. **140**, 171 (2017).
[17] P. E. Dolgirev, I. A. Kruglov, and A. R. Oganov, AIP Adv. **6**, 085318 (2016).
[18] A. P. Bartók and G. Csányi, Int. J. Quantum Chem. **115**, 1051 (2015).
[19] X.-G. Li, C. Hu, C. Chen, Z. Deng, J. Luo, and S. P. Ong, Phys. Rev. B **98**, 094104 (2018).
[20] I. Novoselov, A. Yanilkin, A. Shapeev, and E. Podryabinkin, Comput. Mater. Sci. **164**, 46 (2019).
[21] J. S. Smith, O. Isayev, and A. E. Roitberg, Chem. Sci. **8**, 3192 (2017).
[22] X. Gao, F. Ramezanghorbani, O. Isayev, J. S. Smith, and A. E. Roitberg, J. Chem. Inf. Model. **60**, 3408 (2020).
[23] K. T. Schütt, H. E. Sauceda, P.-J. Kindermans, A. Tkatchenko, and K.-R. Müller, J. Chem. Phys. **148**, 241722 (2018).
[24] T. Segawa, T. Sato, Y. Maruko, and K. Inaki, Silica glass jig for semiconductor industry and method for producing the same, US Patent App. 09/962,918, US 2004/0050102 A1, 2004.
[25] C. Hentzschel, M. Alnaief, I. Smirnova, A. Sakmann, and C. Leopold, Drug. Dev. Ind. Pharm. **38**, 462 (2012).
[26] R. Brady, B. Woonton, M. L. Gee, and A. J. O'Connor, Innov. Food Sci. Emerg. Technol. **9**, 243 (2008).
[27] P. G. Jeelani, P. Mulay, R. Venkat, and C. Ramalingam, Silicon **12**, 1337 (2020).
[28] K. E. Davis, W. B. Russel, and W. J. Glantschnig, Science **245**, 507 (1989).
[29] M. Grzelczak, J. Vermant, E. M. Furst, and L. M. Liz-Marzán, ACS Nano **4**, 3591 (2010).
[30] E. V. Yakovlev, K. A. Komarov, K. I. Zaytsev, N. P. Kryuchkov, K. I. Koshelev, A. K. Zotov, D. A. Shelestov, V. L. Tolstoguzov, V. N. Kurlov, A. V. Ivlev, and S. O. Yurchenko, Sci. Rep. **7**, 13727 (2017).
[31] A. Denoeud, S. Mazevet, F. Guyot, F. Dorchies, J. Gaudin, A. Ravasio, E. Brambrink, and A. Benuzzi-Mounaix, Phys. Rev. E **94**, 031201(R) (2016).

[32] B. B. Karki, D. Bhattarai, and L. Stixrude, Phys. Rev. B **76**, 104205 (2007).
[33] P. K. Hung, N. V. Hong, and L. T. Vinh, J. Phys. Condens. Matter **19**, 466103 (2007).
[34] R. M. Van Ginhoven, H. Jónsson, and L. R. Corrales, Phys. Rev. B **71**, 024208 (2005).
[35] M. Benoit, S. Ispas, P. Jund, and R. Jullien, Eur. Phys. J. B **13**, 631 (2000).
[36] I. Saika-Voivod, F. Sciortino, and P. H. Poole, Phys. Rev. E **63**, 011202 (2000).
[37] M. S. Shell, P. G. Debenedetti, and A. Z. Panagiotopoulos, Phys. Rev. E **66**, 011202 (2002).
[38] H. Niu, P. M. Piaggi, M. Invernizzi, and M. Parrinello, Proc. Natl. Acad. Sci. USA **115**, 5348 (2018).
[39] W. Kob, J. Phys.: Condens. Matter **11**, R85 (1999).
[40] O. B. Tsiok, V. V. Brazhkin, A. G. Lyapin, and L. G. Khvostantsev, Phys. Rev. Lett. **80**, 999 (1998).
[41] Y. D. Fomin, E. N. Tsiok, and V. N. Ryzhov, Phys. Rev. E **87**, 042122 (2013).
[42] Y. Yu, B. Wang, M. Wang, G. Sant, and M. Bauchy, J. Non-Cryst. Solids **443**, 148 (2016).
[43] A. Carré, J. Horbach, S. Ispas, and W. Kob, Europhys. Lett. **82**, 17001 (2008).
[44] S. C. Chowdhury, B. Z. G. Haque, and J. W. Gillespie, J. Mater. Sci. **51**, 10139 (2016).
[45] P. Tangney and S. Scandolo, J. Chem. Phys. **117**, 8898 (2002).
[46] B. W. H. van Beest, G. J. Kramer, and R. A. van Santen, Phys. Rev. Lett. **64**, 1955 (1990).
[47] H. Wang, L. Zhang, J. Han, and W. E, Comput. Phys. Commun. **228**, 178 (2018).
[48] L. Zhang, J. Han, H. Wang, W. Saidi, R. Car, and E. Weinan, in *Advances in Neural Information Processing Systems* (Curran Associates Inc., New York, 2018), pp. 4436–4446.
[49] G. Kresse and J. Furthmuller, Comput. Mater. Sci. **6**, 15 (1996).
[50] J. P. Perdew, J. A. Chevary, S. H. Vosko, K. A. Jackson, M. R. Pederson, D. J. Singh, and C. Fiolhais, Phys. Rev. B **46**, 6671 (1992).
[51] J. P. Perdew and Y. Wang, Phys. Rev. B **45**, 13244 (1992).
[52] G. Kresse and D. Joubert, Phys. Rev. B **59**, 1758 (1999).
[53] S. Plimpton, J. Comput. Phys. **117**, 1 (1995).
[54] D. I. Grimley, A. C. Wright, and R. N. Sinclair, J. Non-Cryst. Solids **119**, 49 (1990).
[55] M. G. Tucker, D. A. Keen, M. T. Dove, and K. Trachenko, J. Phys. Condens. Matter **17**, S67 (2005).
[56] G. C. Sosso, G. Miceli, S. Caravati, J. Behler, and M. Bernasconi, Phys. Rev. B **85**, 174103 (2012).
[57] B. Cheng, E. A. Engel, J. Behler, C. Dellago, and M. Ceriotti, Proc. Natl. Acad. Sci. USA **116**, 1110 (2019).
[58] B. Monserrat, J. G. Brandenburg, E. A. Engel, and B. Cheng, arXiv:2006.13316.
[59] F. Zhang, M. I. Mendelev, Y. Zhang, C.-Z. Wang, M. J. Kramer, and K.-M. Ho, Appl. Phys. Lett. **104**, 061905 (2014).
[60] Y. Zhang, F. Zhang, C. Z. Wang, M. I. Mendelev, M. J. Kramer, and K. M. Ho, Phys. Rev. B **91**, 064105 (2015).
[61] R. E. Ryltsev, B. A. Klumov, N. M. Chtchelkatchev, and K. Y. Shunyaev, J. Chem. Phys. **145**, 034506 (2016).
[62] R. E. Ryltsev, B. A. Klumov, N. M. Chtchelkatchev, and K. Y. Shunyaev, J. Chem. Phys. **149**, 164502 (2018).
[63] D. Gazzillo and G. Pastore, Chem. Phys. Lett. **159**, 388 (1989).
[64] T. S. Grigera and G. Parisi, Phys. Rev. E **63**, 045102(R) (2001).
[65] A. Ninarello, L. Berthier, and D. Coslovich, Phys. Rev. X **7**, 021039 (2017).
[66] N. M. Chtchelkatchev and R. E. Ryltsev, JETP Lett. **102**, 643 (2015).
[67] J.-P. Hansen and I. R. McDonald, *Theory of Simple Liquids*, 4th ed. (Academic Press, San Diego, CA, 2013).
[68] R. E. Ryltsev, N. M. Chtchelkatchev, and V. N. Ryzhov, Phys. Rev. Lett. **110**, 025701 (2013).
[69] N. D. Kondratyuk, G. E. Norman, and V. V. Stegailov, J. Chem. Phys. **145**, 204504 (2016).
[70] G. S. Smirnov and V. V. Stegailov, High Temp. **53**, 829 (2015).
[71] J. Geske, B. Drossel, and M. Vogel, AIP Adv. **6**, 035131 (2016).
[72] http://parallel.uran.ru.